



STUDY OF CRACKING PATTERN AND ITS EVOLUTION ON NATURAL TEXTILE REINFORCED CONCRETE BY IMAGE ANALYSIS

Letícia O. de Souza⁽¹⁾, **Lourdes M.S. de Souza**⁽²⁾ and **Flávio A. Silva**⁽¹⁾

(1) Department of Civil and Environmental Engineering, Pontifícia Universidade Católica do Rio de Janeiro, Brazil

(2) Institute Tecgraf, Pontifícia Universidade Católica do Rio de Janeiro (PUC-Rio), Brazil.

<https://doi.org/10.21452/bccm4.2018.02.09>

Abstract

Textile reinforced concrete (TRC) is an emergent class of material with great deformation capacity and multiple crack formation. Natural fibers are a more eco-friendly alternative to synthetic textile and they are gaining attention in the construction field. In the present study, a Brazilian natural fiber, called curauá, is used in the form of uni-directional textile as reinforcement of cementitious matrix. The composites were manufactured with a hand lay-up technique, varying its thickness and fiber volume fraction. Three types of laminates were investigated under direct tensile tests and its cracking patterns were evaluated by distinct two methodologies. An image processing software was used on photos taken during the tests and a digital image correlation (DIC) technique was also used. The differences between the methods and their limitations are addressed. Parameters as crack spacing and mean crack widths are estimated. The more cracks the composite presented, the more difficult was to perform the measurements due to overlapping of strain fields by DIC. The image analysis performed by the software was able to estimate the number of cracks and the crack spacing for all three types of composites. The mean crack width during the tests was estimated from DIC data.

Keywords: TRC, natural textile, curauá fiber, cement-based composite, image analysis, DIC.

1. INTRODUCTION

Textile reinforced composites (TRC) are a class of materials consist of a fine-grained cementitious matrix reinforced with uni or bi-directional textiles [1,2]. The textile may be of several types, such as carbon, basalt, glass and synthetic fibers [3–5]. Natural fibers are an environmental friendly alternative for textile as they present good strength properties and low cost. Previously works investigated the natural textile capacity of reinforce cementitious matrix, as uni and bi-directional forms [6–9]. An example of uni-directional natural textile reinforced composite is the one developed by Silva et al. [6]: besides the evaluation of the mechanical properties, they investigated the number of cracks and crack spacing of the

composites. The sisal TRC presented mean strength and elastic modulus of 12 and 25 MPa and 34 and 30 GPa, respectively. Image analysis was used and it was found that the crack spacing curve is approximated by an exponential decay function [6].

With improved tensile and ductile properties, TRC are presented as an alternative thin material and may be used for facades and for elements subjected to high strain levels and also for repair. These materials usually present multiple crack formation and their properties are enhanced after the first crack. With that in mind, it is important to understand how cracks behave during the composite loading.

In this work, three types of natural uni-directional TRC are developed and their mechanical responses are studied by means of direct tensile tests. Two distinct methods for investigate crack pattern of the composites during the tensile tests were used: image analysis by acquisition and process of images at regular intervals and digital image correlation (DIC) technique. All the composites presented strain-hardening behavior with multiple crack formation. Their crack pattern was characterized according with the method employed. Besides the parameters obtained with image analysis, DIC also allowed performing an estimation of the mean crack width. This could not be done for all the composites due to cracking characteristics and method's limitation.

2. EXPERIMENTAL PROGRAM

2.1 Materials and process

The curauá fibers used as reinforcement for the composites are obtained from an amazon plant, *Ananas erectifolius*. The strength of curauá is between 250 and 735 MPa [10–12], considered of high performance. Curauá fibers were provided by the CEAPAC organization, from state of Pará, Brazil. The fibers were first cleaned by submersion in hot (around 80°C) tap water for 1 hour. They were dried in an open atmosphere for 48 hours protected from sunlight. Then, they were brushed to be separated into individual filaments. The long and aligned curauá fibers were used as uni-directional textile. They were cut into 500 mm length and assembled into layers of 6.6 g.

One of the main problems of the use of lignocellulosic fibers in cementitious matrix is the durability of the composite. The durability issues are usually caused by alkali attack, fiber mineralization and volume instability [13,14]. The approach used was to reduce the matrix alkalinity by replacing part of the Portland cement by pozzolanic materials. This strategy has proved to be a successful previously [15,16]. In this work, part of Portland cement was replaced by metakaolin and fly ash. The Portland cement used was the Brazilian type CII F-32, metakaolin was obtained from Metacaulim do Brasil Industria e Comercio Ltda and the fly ash from an industry in Santa Catarina – Brazil. The sand used had a maximum diameter of 1.18 mm and density equals to 2.67g/cm³. In order to assure workability, superplasticizer (Glenium 51 (MS)) was used with proportion of 2.5% of the cementitious materials, in weight. The mortar matrix was based on a mix proportion of 1:1:0.4 (cementitious materials:sand:water). The cementitious materials included 50% of Portland cement, 40% of metakaolin and 10% of fly ash, in mass. The mortar was mixed in a 5 L capacity planetary mixer for 1.5 min at 136 rpm and for 4 min at 281 rpm. The resulting matrix presented compressive strength of 54.3 ± 0.5 MPa at 28 days.

The composites were manufactured in a steel mold, intercalating layers of mortar and curauá fibers, starting with a layer of mortar, until reaching the number of layers desired. The dimensions of the laminates were 500 mm (length) by 60 mm (width). The thickness varied with the numbers of layers. It was produced three types of composites with one, three and five fabric layers, resulting in thickness of 6 mm, 11 mm and 14 mm, respectively. The curauá volume fraction was of 4.5%, 7.0% and 8.5% for the composites with one, three and five

layers, respectively. The specimens were covered in their molds for 48 h. Then, they were demolded and cured in water for 26 days.

2.2 Direct tensile test

The specimens were submitted to direct tensile tests. The tests were carried on a servo hydraulic MTS testing machine with closed loop control, model 311.11, with hydraulic wedge grips and load capacity of 1000 kN. Steel plates were added to decrease stress concentration. The tests were performed under displacement control at a rate of 0.1 mm/min. Six specimens with dimensions of 500 mm length were tested of each composite: five for image analysis and one for DIC. The set-up resulted in a fixed-fixed boundary condition. The composites deformations were measured by two LVDTs positioned on the sides of the specimens under a 190 mm gauge length.

2.3 Cracking pattern measurements

After the tests, the specimens were taken under a stereoscope model Nikon SMZ800N to characterize their cracking pattern: number of cracks, cracking space and mean crack width without load applied. The results are the basis for comparison.

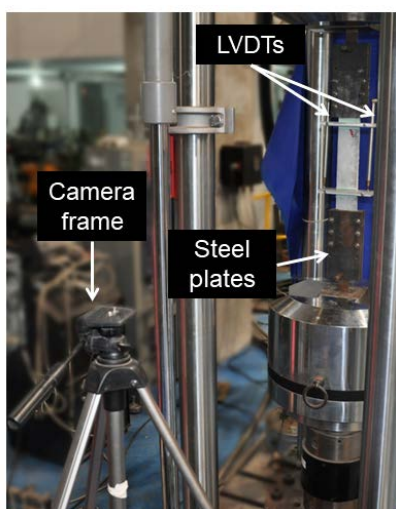
2.3.1 Image analysis

During the tensile tests, a digital camera, model Nikon D90, was placed on a frame grabber directly to the arrangement, as shown in Figure 1-a. The Camera ControlPro2 software was used to capture images of 4200 x 2690 pixels at 10 second intervals. The images with new visible cracks were selected and the space between them was measure by using ImageJ software.

2.3.2 DIC

The DIC is a non-contact and high sensibility technique used in this work to strain field measurements. This method was developed by Sutton et al. [17] and consists of tracking the center of a subset from a reference image to a deformed one. Subsets are groups of pixels and come from a pre-defined area of interest divided into grids. The cross-correlation between the images was performed by the normalized squared differences (NSD) algorithm. The specimens' surfaces were characterized to assure the singularity of each subset, with a high contrast random pattern, as shown in Figure 1-b.

(a)



(b)

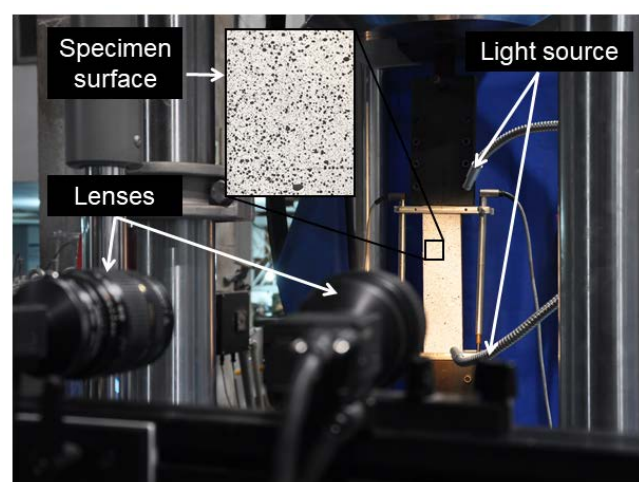


Figure 1: Direct tensile arrangement for (a) image analysis and (b) DIC.

The stereoscope system was formed by two CCD cameras (Point Grey GRAS-50S5M) with resolution of 2448 x 2048 pixels and Tamron A031 (AF28-200mm F/3.8-5.6) lenses. Light sources are used to decrease luminosity variations. The acquisition and processing of images were carried by the software VIC SNAP and VIC-3D 2010, both from Correlated Solutions Inc. The area of interest included 200 mm (from -100 to +100) of the specimens and was divided into 27 subsets. In order to investigate the crack formation, it was plotted strain values versus axial Y position for different test instants. With these information, it was possible to estimate the mean crack width during loading stage.

3. RESULTS AND DISCUSSION

3.1 Tensile response

Figure 2 shows the representative response of the three curauá TRC under direct tensile tests. All the composites presented strain-hardening behavior with multiple crack formation. This behavior is characterized by an elastic linear zone, mostly ruled by the matrix properties due to its major fraction on the composite volume [2]. The deviation of linearity occurs after the first crack and then there is the formation of multiple cracks. More cracks are formed and instead of composite failure, the load bearing capacity is increased due to the cracks bridging by the long curauá fibers. The system is stiff enough to keep the cracks tight until it reaches a steady state condition, marked by the saturation of cracking spacing. Then, there is the widening of the pre-existing cracks: in this zone, no new cracks are formed and it ends when one crack is localized leading to the composite failure. Three and five layered composites presented the above zones well distinguished although this did not occur for the one layered composite.

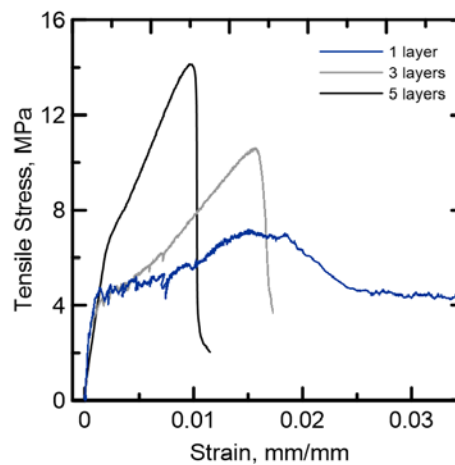


Figure 2: Tensile stress versus strain curves for curauá TRC.

It is possible to observe that the more fiber volume fraction of the composite, the more stiffness it presented as well as ultimate stress. The ultimate strain (correlated with the ultimate stress) decreases with the fiber volume fraction. Thus, the higher ultimate stress, the lower ultimate strain. The drops in the stress-strain response are an indicative of crack formation. The longer the system takes to recover the load bearing capacity, the wider the crack width may be. Thus, the curves in Figure 2 indicate that the mean crack width is decreasing with the higher fiber volume fraction (number of layers). This was confirmed after the tests, with the specimens analyzed under the stereoscope. The resulting crack pattern for the three types of composites is presented on Table 1, as well as the mechanical parameters discussed.

Table 1: Curauá TRC tensile properties and their cracking pattern measured after the tests.

Composite	Mechanical Properties		Measured Cracking Pattern		
	Strength* (MPa)	Strain* (mm/mm)	Number of Cracks	Mean Width (μm)	Crack Spacing (mm)
1 layer	6.3 \pm 0.8	1.2 \pm 0.4	12	42	21.5
3 layers	9.7 \pm 1.4	1.4 \pm 0.1	17	39	13.9
5 layers	14.7 \pm 1.2	1.6 \pm 0.2	56	18	4.2

3.2 Cracking pattern

The image analysis allowed recognition of the number of cracks and the space between them. The DIC method, besides the parameters obtained from image analysis, also allowed an estimated mean crack width. Accuracy and limitations of each method are discussed as follows.

3.2.1 Image analysis

The cracks were time correlated to the strain of each test and the result is shown in Figure 3.

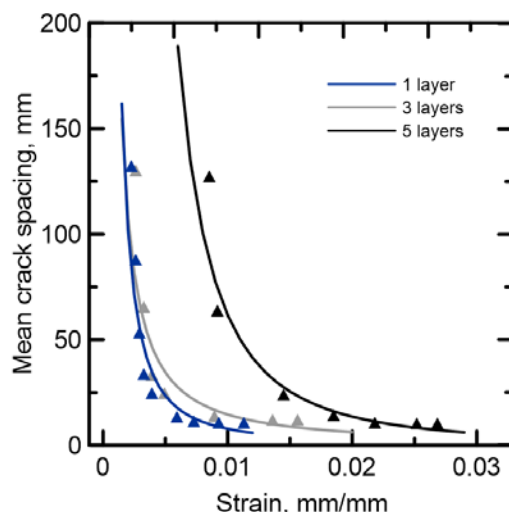


Figure 3: Mean crack spacing measured from image analysis.

It is possible to notice from Figure 3 that the crack evolution of composites reinforced with one and three layers of curauá fabric behave similarly. The mean crack spacing of the five layered composite is shifted around 0.005 mm/mm compared to the other two. This is a result of the difficulty in visualize the cracks initiation, related to its small width. From Table 1, by the end of the test, the mean crack width was of 18 μm , indicating that by the initialization, cracks may be even tighter.

3.2.2 DIC

Table 2 shows the results of the number of visible cracks and the space between them calculated from DIC strain data. The values related with stress level of 4.8 MPa, with correlation of the images, not only strain data. The DIC method could not contemplate five layered composite analysis due to the crack overlapping (red rectangles in Figure 4). This lead to complications on separating cracks near to each other.

From Figure 4, it is possible to observe that each peak on strain curve is a reasonable approximation of one crack. The same did not happen to the five layered composite, since the cracks are closely spaced (see Table 1). Combining both DIC data and images from the test, it

was possible to make an estimate of crack width evolution for different instants of the tests and correlate them with stress levels, as shown in Figure 5. Those values are an approximation due to limitations of the method, since the resolution is 60 microstrains.

Table 2: Crack pattern from DIC analysis.

Composite	N° of cracks	Mean crack spacing (mm)	Mean crack width* (μm)
1 layer	7	22.5	337
3 layers	11	15.7	122
5 layers	26	5.8	19

* Values related to stress level of 4.8 MPa.

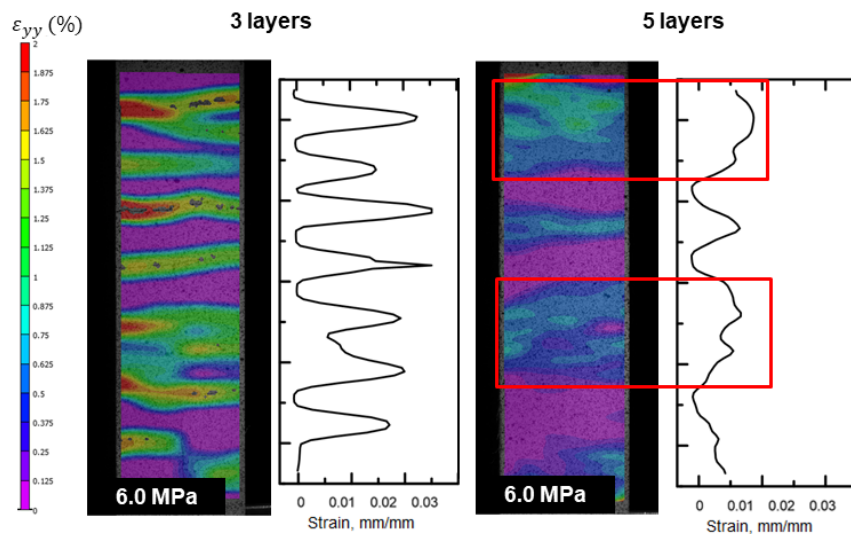


Figure 4: Comparison between DIC data for three and five layered composites. Red rectangles indicating overlapping in strain curve.

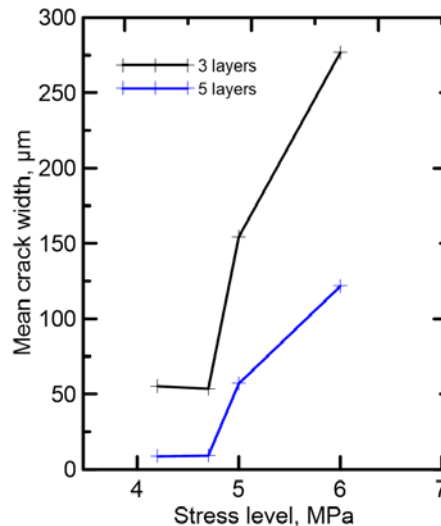


Figure 5: Mean crack width evolution during tensile test, for three and five layered composites.

4. CONCLUSIONS

Curauá uni-directional textile was able to reinforce cementitious composites and provide them of strain-hardening behavior even for the ones with fiber fraction of 4.5%.

The image analysis was able to estimate the number of cracks and the crack spacing and the results are in good agreement with the values measured with the stereoscope. The DIC analysis resulted in crack spacing measurements in good accordance with the real one for the one and three layers types of composites. The same did not happen with the five layered composite due to cracks overlapping since they are closely spaced, mostly for stress level above 5 MPa. The mean crack width during the tests was estimated by combining DIC data and images taken during the tests.

ACKNOWLEDGEMENTS

The authors gratefully acknowledge the CNPq and CAPES (Brazilian National Science Foundations) for partial financial support for this work.

REFERENCES

- [1] Textile Reinforced Concrete, State-of-the-Art Report of RILEM Technical Committee 201-TRC., Bagnex, France, 2006.
- [2] B. Mobasher, Mechanics of fiber and textile reinforced cement composites, 2012.
- [3] F.D.A. Silva, M. Butler, S. Hempel, R.D. Toledo Filho, V. Mechtcherine, Effects of elevated temperatures on the interface properties of carbon textile-reinforced concrete, *Cem. Concr. Compos.* 48 (2014) 26–34. doi:10.1016/j.cemconcomp.2014.01.007.
- [4] D. Alan, S. Rambo, F.D.A. Silva, R. Dias, T. Filho, P.O. Box, R. De Janeiro, Effect of high temperature on the behavior of basalt textile reinforced refractory concrete under uniaxial tensile loading, 1 (2014).
- [5] F. de A. Silva, M. Butler, V. Mechtcherine, D. Zhu, B. Mobasher, Strain rate effect on the tensile behaviour of textile-reinforced concrete under static and dynamic loading, *Mater. Sci. Eng. A.* 528 (2011) 1727–1734. doi:10.1016/j.msea.2010.11.014.
- [6] F. de A. Silva, B. Mobasher, R.D.T. Filho, Cracking mechanisms in durable sisal fiber reinforced cement composites, *Cem. Concr. Compos.* 31 (2009) 721–730. doi:10.1016/j.cemconcomp.2009.07.004.
- [7] J. Claramunt, L.J. Fernández-carrasco, H. Ventura, M. Ardanuy, Natural fiber nonwoven reinforced cement composites as sustainable materials for building envelopes, 115 (2016) 230–239. doi:10.1016/j.conbuildmat.2016.04.044.
- [8] A. Hakamy, F.U.A. Shaikh, I.M. Low, Characteristics of hemp fabric reinforced nanoclay – cement nanocomposites, *Cem. Concr. Compos.* 50 (2014) 27–35. doi:10.1016/j.cemconcomp.2014.03.002.
- [9] M.E.A. Fidelis, F. de A. Silva, R.D.T. Filho, The Influence of Fiber Treatment on the Mechanical Behavior of Jute Textile Reinforced Concrete, *Key Eng. Mater.* 600 (2014) 469–474. doi:10.4028/www.scientific.net/KEM.600.469.
- [10] M.A.S. Spinacé, C.S. Lambert, K.K.G. Feroselli, M. De Paoli, Characterization of lignocellulosic curaua fibres, *Carbohydr. Polym.* 77 (2009) 47–53. doi:10.1016/j.carbpol.2008.12.005.
- [11] F. Tomczak, K.G. Satyanarayana, T.H.D. Sydenstricker, Studies on lignocellulosic fibers of Brazil : Part III – Morphology and properties of Brazilian curauá fibers, *Compos. Part A Appl. Sci. Manuf.* 38 (2007) 2227–2236. doi:10.1016/j.compositesa.2007.06.005.
- [12] D.G. Soltan, P. das Neves, A. Olvera, H. Savastano Junior, V.C. Li, Introducing a curauá fiber reinforced cement-based composite with strain-hardening behavior, *Ind. Crops Prod.* 103 (2017) 1–12. doi:10.1016/j.indcrop.2017.03.016.
- [13] R.D.T. Filho, K. Scrivener, G.L. England, K. Ghavami, Durability of alkali-sensitive sisal and coconut fibres in cement mortar composites, *Cem. Concr. Compos.* 22 (2000) 127–143.
- [14] R.D.T. Filho, F. de A. Silva, E.M.R. Fairbairn, J. de A.M. Filho, Durability of compression molded sisal fiber reinforced mortar laminates, *Constr. Build. Mater.* 23 (2009) 2409–2420. doi:10.1016/j.conbuildmat.2008.10.012.
- [15] R.D.T. Filho, K. Ghavami, G.L. England, K. Scrivener, Development of vegetable fibre – mortar composites of improved durability, *Cem. Concr. Compos.* 25 (2003) 185–196.

- [16] J. Wei, C. Meyer, Degradation mechanisms of natural fiber in the matrix of cement composites, *Cem. Concr. Res.* 73 (2015) 1–16. doi:<http://dx.doi.org/10.1016/j.cemconres.2015.02.019>.
- [17] M.A. Sutton, J.L. Turner, H.A. Bruck, T.A. Chae, Full field Representation of Discretely Sampled Surface Deformation for Displacement and Strain Analysis, *Exp. Mech.* (1991) 168–177.